



Gilbert damping in metallic ferromagnets from Schwinger-Keldysh field theory: Intrinsically nonlocal, nonuniform, and made anisotropic by spin-orbit coupling

Felipe Reyes-Osorio  and Branislav K. Nikolić ^{*}

Department of Physics and Astronomy, University of Delaware, Newark, Delaware 19716, USA



(Received 20 September 2023; revised 8 December 2023; accepted 11 December 2023; published 12 January 2024)

Understanding the origin of damping mechanisms in the magnetization dynamics of metallic ferromagnets is a fundamental problem for nonequilibrium many-body physics of systems in which quantum conduction electrons interact with localized spins assumed to be governed by the classical Landau-Lifshitz-Gilbert (LLG) equation. It is also of critical importance for applications because damping affects energy consumption and the speed of spintronic and magnonic devices. Since the 1970s, a variety of linear-response and scattering theory approaches have been developed to produce widely used formulas for computation of the spatially independent Gilbert scalar parameter as the magnitude of the Gilbert damping term in the LLG equation. The Schwinger-Keldysh field theory (SKFT), largely unexploited for this purpose, offers additional possibilities, such as to rigorously derive an extended LLG equation by integrating quantum electrons out. Here we derive such an equation whose Gilbert damping for metallic ferromagnets is *nonlocal*, i.e., dependent on all localized spins at a given time, and *nonuniform*, even if all localized spins are collinear and spin-orbit coupling (SOC) is absent. This is in sharp contrast to standard lore, in which nonlocal damping is considered to emerge only if localized spins are noncollinear—for such situations, direct comparison using the example of a magnetic domain wall shows that SKFT-derived nonlocal damping is an order of magnitude larger than the previously considered one. Switching on SOC makes such nonlocal damping *anisotropic*, in contrast to standard lore, in which SOC is usually necessary to obtain a nonzero Gilbert damping scalar parameter. Our analytical formulas, with their nonlocality being more prominent in low spatial dimensions, are fully corroborated by numerically exact quantum-classical simulations.

DOI: [10.1103/PhysRevB.109.024413](https://doi.org/10.1103/PhysRevB.109.024413)

I. INTRODUCTION

The celebrated Landau-Lifshitz equation [1] is the foundation of standard frameworks, such as classical micromagnetics [2,3] and atomistic spin dynamics [4], for modeling the dynamics of local magnetization within magnetic materials driven by external fields or currents in spintronics [2] and magnonics [3]. It considers localized spins to be classical vectors $\mathbf{M}(\mathbf{r})$ of fixed length normalized to unity whose rotation around the effective magnetic field \mathbf{B}_{eff} is governed by

$$\partial_t \mathbf{M} = -\mathbf{M} \times \mathbf{B}_{\text{eff}} + \mathbf{M} \times (\mathcal{D} \cdot \partial_t \mathbf{M}), \quad (1)$$

where $\partial_t \equiv \partial/\partial t$. Although spin is a genuine quantum degree of freedom, such a phenomenological equation can be fully microscopically justified from open quantum many-body system dynamics in which $\mathbf{M}(\mathbf{r})$ tracks the trajectories of the quantum-mechanical expectation values of localized spin operators [5] in ferromagnets, as well as in antiferromagnets as long as the spin value is sufficiently large, $S > 1$. The presence of a dissipative environment in this justification invariably introduces damping mechanisms, which were phenomenologically conjectured in the earliest formulation [1], as well as in later renderings using the so-called Gilbert form of damping [6,7], written as the second term on the right-hand side (RHS) of Eq. (1).

The Gilbert damping \mathcal{D} was originally considered a spatially uniform scalar $\mathcal{D} \equiv \alpha_G$ or possibly tensor [8,9], depending on the intrinsic properties of a material. Its typical values are $\alpha_G \sim 0.01$ in standard ferromagnetic metals [10] and as low as $\alpha_G \sim 10^{-4}$ in carefully designed magnetic insulators [11] and metals [12]. Furthermore, recent extensions [13–21] of the Landau-Lifshitz-Gilbert (LLG) equation (1) to the dynamics of noncollinear magnetization textures found \mathcal{D} to be a spatially nonuniform and nonlocal tensor,

$$\mathcal{D}_{\alpha\beta} = \alpha_G \delta_{\alpha\beta} + \eta \sum_{\beta'} (\mathbf{M} \times \partial_{\beta'} \mathbf{M})_{\alpha} (\mathbf{M} \times \partial_{\beta'} \mathbf{M})_{\beta}, \quad (2)$$

where $\partial_{\beta'} \equiv \partial/\partial \beta'$ and $\alpha, \beta, \beta' \in \{x, y, z\}$.

It is generally believed that α_G is *nonzero only* when spin-orbit coupling (SOC) [22,23], magnetic disorder or both are present [15,24,25]. For example, α_G was extracted from a nonrelativistic expansion of the Dirac equation [22,23], and SOC is virtually always invoked in analytical (conducted for simplistic model Hamiltonians) [26–28] or first-principles calculations [24,25,29–33] of α_G via Kubo linear-response [9,30,34–36] or scattering [8] theory formulas.

The second term on the RHS of Eq. (2) is the particular form [13] of the so-called *nonlocal* (i.e., magnetization-texture-dependent) and *spatially nonuniform* (i.e., position-dependent) damping [13–21,37]. The search for a proper form of nonlocal damping has a long history [19,37]. Its importance was revealed by experiments [10] extracting very different

^{*}bnikolic@udel.edu

Gilbert dampings for the same material by using its uniformly precessing localized spins versus the dynamics of its magnetic domain walls, as well as in experiments observing wave-vector-dependent damping of spin waves [38]. Its particular form [13] in Eq. (2) *requires* only noncollinear and noncoplanar textures of localized spins, so it can be nonzero even in the absence of SOC, but the presence of SOC can greatly enhance its magnitude [18] (without SOC, the nonlocal damping in Eq. (2) is estimated [18] to be relevant only for small, $\lesssim 1$ nm, noncollinear magnetic textures).

However, recent quantum-classical and numerically exact simulations [39,40] revealed that α_G can be nonzero even in the absence of SOC simply because the expectation value of the conduction electron spin $\langle \hat{s}_n \rangle$ *always lags behind* \mathbf{M}_n . This retarded response of electronic spins with respect to the motion of classical localized spins, also invoked when postulating the extended LLG equation with a phenomenological time-retarded kernel [41], generates spin torque $\propto \langle \hat{s}_n \rangle \times \mathbf{M}_n$ [42] and thereby effective Gilbert-like damping [39–41] that is nonzero in the absence of SOC and operative even if \mathbf{M}_n at different sites n are *collinear* [40]. Including SOC in such simulations simply increases [43] the angle between $\langle \hat{s}_n \rangle$ and \mathbf{M}_n and therefore the effective damping.

Deepening our understanding of the origin of these phenomena observed in numerical simulations, which are analogous to the nonadiabatic effects discussed in diverse fields in which fast quantum degrees of freedom interact with slow classical ones [44–47], requires deriving an analytical expression for Gilbert damping due to the interaction between fast conduction electrons and slow localized spins. A rigorous path for this derivation is offered by the Schwinger-Keldysh nonequilibrium field theory (SKFT) [48], which, however, remains largely unexplored for this problem. We note that a handful of studies have employed SKFT to study small systems of one or two localized spins [49–54] as they interact with conduction electrons. While some of these studies [49,53,54] also arrived at an extended LLG equation with nonlocal damping, they are directly applicable to only small magnetic molecules rather than the macroscopic ferromagnets that are the focus of our study. It is also worth mentioning that an early work [55] did apply SKFT to the same model we are using—electrons whose spins interact via sd exchange interaction with many Heisenberg-exchange-coupled localized spins representing a metallic ferromagnet in a self-consistent manner—but the authors did not obtain a damping term in their extended Landau-Lifshitz equation and instead focused on fluctuations in the magnitude of \mathbf{M}_n . In contrast, the vectors \mathbf{M}_n are of fixed length in classical micromagnetics [2,3] and atomistic spin dynamics [4], as well as in our SKFT-derived extended LLG equation (9) and all other SKFT-based analyses of one or two localized spin problems [49–54].

In this study we consider either an infinite metallic magnet [Fig. 1(a)] or a finite one [Fig. 1(b)] sandwiched between two semi-infinite normal metal (NM) leads terminating in macroscopic electronic reservoirs [8,52,53], whose localized spins are coupled by ferromagnetic exchange in equilibrium. The setups in Fig. 1 have direct relevance to experiments [10,38] on external field [Fig. 1(a)] or current-driven dynamics [Fig. 1(b)] of localized spins in spintronics and magnonics. Our principal result is encapsulated by Fig. 1(c): Gilbert

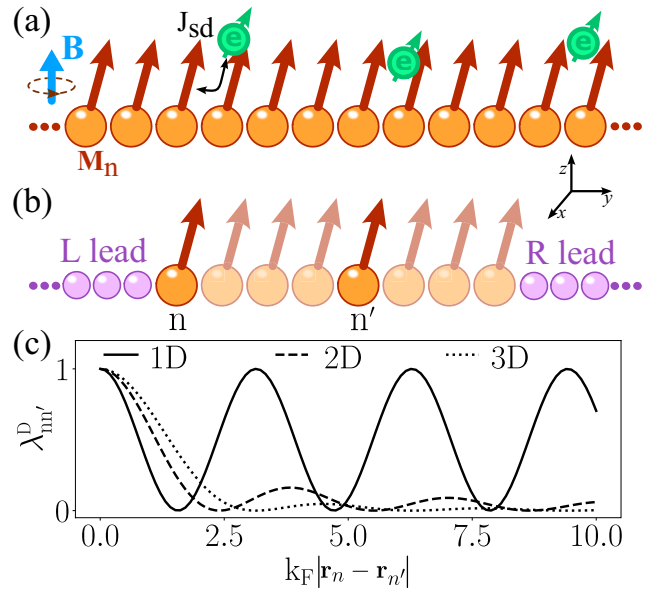


FIG. 1. Schematic view of (a) classical localized spins, modeled by unit vectors \mathbf{M}_n (red arrows), within an infinite metallic ferromagnet defined on a cubic lattice in one to three dimensions (one dimension is used in this illustration) and (b) a finite-size metallic ferromagnet (central region) attached to semi-infinite NM leads terminating in macroscopic reservoirs, whose difference in electrochemical potentials injects charge current, as commonly done in spintronics. The localized spins interact with conduction electron spin $\langle \hat{s} \rangle$ (green arrow) via sd exchange of strength J_{sd} , while both subsystems can experience external magnetic field \mathbf{B} (blue arrow). (c) Nonlocal damping $\lambda_{nn'}^D$ [Eq. (10)] obtained from SKFT vs the distance $|\mathbf{r}_n - \mathbf{r}_{n'}|$ between two sites n and n' of the lattice for different dimensionalities D of space.

damping due to conduction electron spins lagging behind the classical localized ones which is nonlocal and inhomogeneous, with such features becoming more prominent in low-dimensional ferromagnets. This result is independently confirmed (Fig. 2) in one dimension by numerically exact simulations based on the time-dependent nonequilibrium Green's function combined with the LLG equation (TDNEGF+LLG) scheme [40,43,56,57].

We note that conventional linear-response formulas [9,30,34–36] produce unphysical divergent Gilbert damping [33] in a perfectly crystalline magnet at zero temperature. In contrast to previously proposed solutions to this problem, which require [58–60] going beyond the standard picture of electrons that do not interact with each other while interacting with classical localized spins, our formulas are finite in the clean limit, as well as in the absence of SOC. Scattering theory [8] yields a formula for α_G which is also always finite (in the absence of SOC, it is finite due to spin pumping [61]). However, that result can be viewed only as a spatial average of our nonlocal damping, which cannot produce proper LLG dynamics of local magnetization (Fig. 3).

This paper is organized as follows. In Sec. II we formulate the SKFT approach to the dynamics of localized spins interacting with conduction electrons within a metallic ferromagnet. Sections III A and III B show how this approach

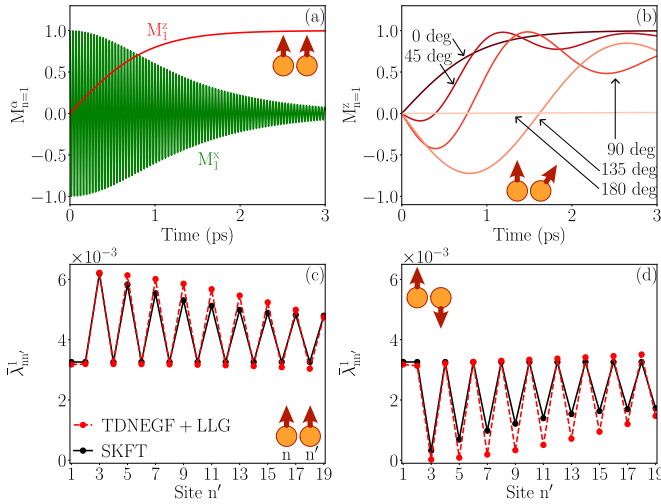


FIG. 2. (a) Time evolution of two localized spins \mathbf{M}_n , located at sites $n = 1$ and $n' = 3$ within a chain of 19 sites in the setup of Fig. 1(b), computed numerically using the TDNEGF+LLG scheme [40,43,56,57]. The two spins are collinear at $t = 0$ and point along the x axis, while magnetic field is applied along the z axis. (b) The same information as in (a), but for two noncollinear spins with angle $\in \{0, 45, 90, 135, 180\}$ between them. (c) and (d) Effective damping extracted from TDNEGF+LLG simulations (red dashed line) vs the one from SKFT [the black solid line plots the 1D case in Eq. (10)] as a function of the site n' of the second spin. The two spins are initially parallel in (c) and antiparallel in (d). The Fermi wave vector of conduction electrons is chosen to be $k_F = \pi/2a$, where a is the lattice spacing.

leads to nonlocal and isotropic or nonlocal and anisotropic damping in the presence or absence of SOC, respectively. The SKFT-derived analytical results are corroborated by numerically exact TDNEGF+LLG simulations [40,43,56,57] in Sec. III C. Then, in Secs. III D and III E we compare SKFT-derived formulas with the widely used scattering theory of conventional scalar Gilbert damping [8,61,62] and spin-motive force (SMF) theory [13,19] of nonlocal damping. Finally, in Sec. III F, we discuss how to combine our SKFT-derived formulas with first-principles calculations of realistic materials via density functional theory (DFT). We conclude in Sec. IV.

II. SCHWINGER-KELDYSH FIELD THEORY FOR METALLIC FERROMAGNETS

The starting point of SKFT is the action [48] of the metallic ferromagnet, $S = S_M + S_e$,

$$S_M = \int_C dt \sum_n \{ \partial_t \mathbf{M}_n(t) \cdot \mathbf{A}_n - \mathcal{H}[\mathbf{M}_n(t)] \}, \quad (3a)$$

$$S_e = \int_C dt \sum_{nn'} [\bar{\psi}_n(t) (i\partial_t - \gamma_{nn'}) \psi_{n'}(t) - \delta_{nn'} J_{sd} \mathbf{M}_n(t) \cdot \mathbf{s}_{n'}(t)], \quad (3b)$$

where S_M is the contribution from localized spins and S_e is the contribution from conduction electrons. The integration \int_C is along the Keldysh closed contour \mathcal{C} [48]. Here the subscript n labels the site of a D -dimensional cubic lattice;

$\partial_t \mathbf{M}_n \cdot \mathbf{A}_n$ is the Berry phase term [63,64]; $\mathcal{H}[\mathbf{M}_n]$ is the Hamiltonian of localized spins; $\psi_n = (\psi_n^\uparrow, \psi_n^\downarrow)^T$ is the Grassmann spinor [48] for an electron at site n ; $\gamma_{nn'} = -\gamma$ is the nearest-neighbor (NN) hopping; $\mathbf{s}_n = \bar{\psi}_n \boldsymbol{\sigma} \psi_n$ is the electronic spin density, where $\boldsymbol{\sigma}$ is the vector of the Pauli matrices; and J_{sd} is the magnitude of the sd exchange interaction between flowing spins of conduction electrons and localized spins. For simplicity, we use $\hbar = 1$.

The Keldysh contour \mathcal{C} , as well as all functions defined on it, can be split into forward (+) and backward (−) segments [48]. These functions can, in turn, be rewritten as $\mathbf{M}_n^\pm = \mathbf{M}_{n,c} \pm \frac{1}{2} \mathbf{M}_{n,q}$ for the real-valued localized spins field, and $\psi_n^\pm = \frac{1}{\sqrt{2}} (\psi_{1,n} \pm \psi_{2,n})$ and $\bar{\psi}_n^\pm = \frac{1}{\sqrt{2}} (\bar{\psi}_{2,n} \pm \bar{\psi}_{1,n})$ for the Grassmann-valued fermion fields ψ_n and $\bar{\psi}_n$. The subscripts c and q refer to the classical and quantum components of time evolution. This rewriting yields the following expressions for the two actions:

$$S_M = \int dt \sum_n M_{nq}^\alpha (\epsilon_{\alpha\beta\gamma} \partial_t M_{n,c}^\beta M_{n,c}^\gamma + B_{\text{eff}}^\alpha [\mathbf{M}_{n,c}]), \quad (4a)$$

$$S_e = \int dt dt' \sum_{nn'} \bar{\psi}_n^\sigma (\check{G}_{nn'}^{-1} \delta_{\sigma\sigma'} - J_{sd} \check{M}_{nn'}^\alpha \sigma_{\sigma\sigma'}^\alpha) \psi_{n'}^{\sigma'}, \quad (4b)$$

where the subscript $\sigma = \uparrow, \downarrow$ indicates spin; summation over repeated Greek indices is implied; $\boldsymbol{\psi} \equiv (\psi_1, \psi_2)^T$; $\mathbf{B}_{\text{eff}} = -\delta\mathcal{H}/\delta\mathbf{M}$ is the effective magnetic field; $\epsilon_{\alpha\beta\gamma}$ is the Levi-Civita symbol; and \check{O} are 2×2 matrices in the Keldysh space, such as

$$\check{G}_{nn'}^R = \begin{pmatrix} G^R & G^K \\ 0 & G^A \end{pmatrix}_{nn'}, \quad \check{M}_{nn'}^\alpha = \begin{pmatrix} M_c & \frac{M_q}{2} \\ \frac{M_q}{2} & M_c \end{pmatrix}_n^\alpha \delta_{nn'}. \quad (5)$$

Here $G_{nn'}^{R/A/K}(t, t')$ are electronic retarded/advanced/Keldysh Green's functions (GFs) [48] in the real-space representation of sites n .

The electrons can be integrated out [49] up to the second order in J_{sd} coupling, thereby yielding an effective action for only localized spins,

$$S_M^{\text{eff}} = \int dt \sum_n M_{n,q}^\alpha \left\{ \epsilon_{\alpha\beta\gamma} \partial_t M_{n,c}^\beta M_{n,c}^\gamma + B_{\text{eff}}^\alpha [\mathbf{M}_{n,c}] + \int dt' \sum_{n'} M_{n',c}^\alpha(t') \eta_{nn'}(t, t') \right\}, \quad (6)$$

where

$$\eta_{nn'}(t, t') = iJ_{sd}^2 [G_{nn'}^R(t, t') G_{nn'}^K(t', t) + G_{nn'}^K(t, t') G_{nn'}^A(t', t)] \quad (7)$$

is the non-Markovian time-retarded kernel. Note that terms that are second order in the quantum fluctuations $\mathbf{M}_{n,q}$ are neglected [48] in order to write Eq. (6). The magnetization damping can be explicitly extracted by analyzing the kernel, as demonstrated for different ferromagnetic setups in Secs. III A and III B.

III. RESULTS AND DISCUSSION

A. Nonlocality of Gilbert damping in metallic ferromagnets in the absence of SOC

Since $\eta_{nn'}(t - t')$ depends only on the difference $t - t'$, it can be Fourier transformed to energy ε . Thus, the kernel can be written explicitly for low energies as

$$\eta_{nn'}(\varepsilon) = J_{sd}^2 \frac{i\varepsilon}{2\pi} \sum_{\mathbf{k}, \mathbf{q}} e^{i\mathbf{k} \cdot (\mathbf{r}_n - \mathbf{r}_{n'})} e^{i\mathbf{q} \cdot (\mathbf{r}_n - \mathbf{r}_{n'})} A_{\mathbf{k}}(\mu) A_{\mathbf{q}}(\mu), \quad (8)$$

where $A_{\mathbf{k}}(\mu) \equiv i[G_{\mathbf{k}}^R(\mu) - G_{\mathbf{k}}^A(\mu)]$ is the spectral function [52] evaluated at chemical potential μ , \mathbf{k} is a wave vector, and \mathbf{r}_n and $\mathbf{r}_{n'}$ are the position vectors of sites n and n' . Equation (8) remains finite in the clean limit and for low temperatures, so it evades unphysical divergences in the linear-response approaches [58–60]. By transforming it back into the time domain, we minimize the effective action in Eq. (6) with respect to the quantum fluctuations to obtain semiclassical equations of motion for classical localized spins. This procedure is equivalent to the so-called large-spin approximation [65,66] or a one-loop truncation of the effective action. The higher-order terms neglected in Eq. (6) contribute a stochastic noise that vanishes in the low-temperature and large-spin limit. Although the fluctuating effect of this noise can modify the exact dynamics [54,65], the deterministic regime suffices for a qualitative understanding and is often the main focus of interest [66,67].

Thus, we arrive at the following extended LLG equation:

$$\partial_t \mathbf{M}_n = -\mathbf{M}_n \times \mathbf{B}_{\text{eff},n} + \mathbf{M}_n \times \sum_{n'} \lambda_{nn'}^D \partial_t \mathbf{M}_{n'}, \quad (9)$$

where the conventional $\alpha_G \mathbf{M}_n \times \partial_t \mathbf{M}_n$ Gilbert term is replaced by the second term on the RHS exhibiting nonlocal damping $\lambda_{nn'}^D$ instead of the Gilbert damping scalar parameter α_G . A closed expression for $\lambda_{nn'}^D$ can be obtained for one-dimensional (1D), two-dimensional (2D), and three-

dimensional (3D) metallic ferromagnets by considering the quadratic energy-momentum dispersion of their conduction electrons:

$$\lambda_{nn'}^D = \begin{cases} \frac{2J_{sd}^2}{\pi v_F^2} \cos^2(k_F |\mathbf{r}_n - \mathbf{r}_{n'}|) & 1\text{D}, \\ \frac{k_F^2 J_{sd}^2}{2\pi v_F^2} J_0^2(k_F |\mathbf{r}_n - \mathbf{r}_{n'}|) & 2\text{D}, \\ \frac{k_F^2 J_{sd}^2}{2\pi v_F^2} \frac{\sin^2(k_F |\mathbf{r}_n - \mathbf{r}_{n'}|)}{|\mathbf{r}_n - \mathbf{r}_{n'}|^2} & 3\text{D}. \end{cases} \quad (10)$$

Here k_F is the Fermi wave vector of electrons, v_F is their Fermi velocity, and $J_0(x)$ is the zeroth Bessel function of the first kind.

B. Nonlocality and anisotropy of Gilbert damping in metallic ferromagnets in the presence of SOC

Taking into account that previous analytical calculations [26–28] of the conventional Gilbert damping scalar parameter always included SOC, often of the Rashba type [68], in this section we show how to generalize Eq. (8) and nonlocal damping extracted in the presence of SOC. For this purpose, we employ the Rashba Hamiltonian in one dimension, with its diagonal representation given by $\hat{H} = \sum_{k\sigma} \varepsilon_{k\sigma} \hat{c}_{k\sigma}^\dagger \hat{c}_{k\sigma}$, where $\hat{c}_{k\sigma}^\dagger$ ($\hat{c}_{k\sigma}$) creates (annihilates) an electron with wave number k and spin σ oriented along the y axis, $\varepsilon_{k\sigma} = -2\gamma \cos k + 2\sigma \gamma_{\text{SO}} \sin k$ is the Rashba spin-split energy-momentum dispersion, and γ_{SO} is the strength of the Rashba SOC coupling. By switching from second-quantized operators $\hat{c}_{k\sigma}^\dagger$ and $\hat{c}_{k\sigma}$ to Grassmann-valued two-component fields [64] $\tilde{\mathbf{c}}_n^\sigma$ and \mathbf{c}_n^σ , where $\mathbf{c}_n^\sigma = (c_{1,n}^\sigma, c_{2,n}^\sigma)^T$, we obtain, for the electronic action,

$$S_e = \int dt dt' \sum_{nn'} \tilde{\mathbf{c}}_n^\sigma [(\check{G}_{nn'}^\sigma)^{-1} \delta_{\sigma\sigma'} - J_{sd} \check{M}_{nn'}^\alpha \sigma_{\sigma\sigma'}^\beta] \mathbf{c}_{n'}^{\sigma'}. \quad (11)$$

Here $\check{G}_{nn'}^\sigma$ is diagonal, but it depends on spin through $\varepsilon_{k\sigma}$. In addition, $\check{M}_{nn'}^{\alpha,x,y,z}$, as the matrix which couples to the same $\sigma^{x,y,z}$ Pauli matrix in the electronic action without SOC [Eq. (3b)], is coupled in Eq. (11) to a different Pauli matrix $\sigma^{y,z,x}$.

By integrating electrons out up to the second order in J_{sd} and repeating steps analogous to those in Sec. II while carefully differentiating the spin-split bands, we find that nonlocal damping becomes anisotropic:

$$\lambda_{nn'}^{1\text{D}} = \begin{pmatrix} \alpha_{nn'}^\perp & 0 & 0 \\ 0 & \alpha_{nn'}^\parallel & 0 \\ 0 & 0 & \alpha_{nn'}^\perp \end{pmatrix}, \quad (12)$$

where

$$\alpha_{nn'}^\perp = \frac{J_{sd}^2}{\pi} \left(\frac{\cos^2(k_F^\uparrow |\mathbf{r}_n - \mathbf{r}_{n'}|)}{v_F^{\uparrow 2}} + \frac{\cos^2(k_F^\downarrow |\mathbf{r}_n - \mathbf{r}_{n'}|)}{v_F^{\downarrow 2}} \right), \quad (13a)$$

$$\alpha_{nn'}^\parallel = \frac{J_{sd}^2}{\pi |v_F^\uparrow v_F^\downarrow|} \{ \cos[(k_F^\uparrow + k_F^\downarrow) |\mathbf{r}_n - \mathbf{r}_{n'}|] + \cos[(k_F^\uparrow - k_F^\downarrow) |\mathbf{r}_n - \mathbf{r}_{n'}|] \}, \quad (13b)$$

and $k_F^{\uparrow/\downarrow}$ and $v_F^{\uparrow/\downarrow}$ are the Fermi wave vectors and velocities, respectively, of the Rashba spin-split bands. This means that the damping term in Eq. (9) is now given by $\mathbf{M}_n \times \sum_{n'} \lambda_{nn'}^{1\text{D}} \cdot \partial_t \mathbf{M}_{n'}$.

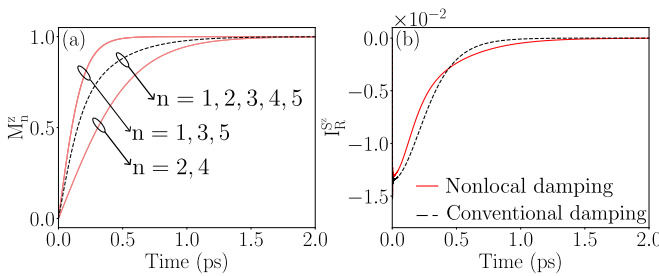


FIG. 3. (a) Comparison of trajectories of localized spins $M_n^z(t)$ in the setup in Fig. 1(b), whose central region is a 1D metallic ferromagnet composed of five sites, using LLG equation (9) with SKFT-derived nonlocal damping (solid red lines) vs the LLG equation with conventional spatially independent $\alpha_G = 0.016$ (black dashed line). This value of α_G is obtained by averaging nonlocal damping over the whole ferromagnet. The dynamics of $\mathbf{M}_n(t)$ is initiated by an external magnetic field along the z axis, while all five localized spins point along the x axis at $t = 0$. (b) Comparison of spin current $I_R^z(t)$ pumped [56,57,61] by the dynamics of $\mathbf{M}_n(t)$ for the two cases [i.e., nonuniform $\mathbf{M}_n(t)$ for nonlocal damping vs uniform $\mathbf{M}_n(t)$ for conventional damping] from (a). The Fermi wave vector of conduction electrons is chosen to be $k_F = \pi/2a$.

We note that previous experimental [69], numerical [9,70], and analytical [26–28] studies also found SOC-induced anisotropy of the Gilbert damping scalar parameter. However, our results [Eqs. (12) and (13)] exhibit the additional features of nonlocality (i.e., damping at site n depends on spin at site n') and nonuniformity (i.e., dependence on $|\mathbf{r}_n - \mathbf{r}_{n'}|$). As expected from Sec. III A, nonlocality persists for $\gamma_{\text{SO}} = 0$, i.e., $k_F^\uparrow = k_F^\downarrow = k_F$, with $\lambda_{nn'}^{\text{1D}}$ properly reducing to contain three equal diagonal elements. Additionally, the damping component $\alpha_{nn'}^{\parallel}$ given by Eq. (13b) can take negative values, revealing the driving capability of the conduction electrons (see Sec. III C). However, for realistic small values of γ_{SO} , the driving contribution of nearby localized spins is likewise small. Furthermore, the decay of nonlocal damping with increasing distance observed in two and three dimensions, together with the presence of intrinsic local damping from other sources, ensures that the system tends toward equilibrium.

C. Comparison of SKFT-derived formulas with numerically exact TDNEGF+LLG simulations

An analytical solution to Eq. (9) can be obtained in a few special cases, such as for two exchange-uncoupled localized spins at sites $n = 1$ and $n' \neq 1$ within a 1D wire placed in an external magnetic field $\mathbf{B}_{\text{ext}} = B_{\text{ext}}\mathbf{e}_z$, with the proviso that the two spins are collinear at $t = 0$. The same system can be simulated by the TDNEGF+LLG scheme, so that comparing the analytical solution to such a numerically exact solution for trajectories $\mathbf{M}_n(t)$ makes it possible to investigate the accuracy of our derivation and approximations involved in it, such as truncation to J_{sd}^2 order, keeping quantum fluctuations $\mathbf{M}_{n,q}$ to first order, and low-energy approximation used in Eq. (8). While such a toy model is employed to verify the SKFT-based derivation, we note that two uncoupled localized spins can also be interpreted as macrospins of two distant ferromagnetic layers within a spin valve for which oscillatory Gilbert damping as a function of distance between the layers was observed experimentally [71]. Note that semi-infinite NM leads from the setup in Fig. 1(b), which are always used in TDNEGF+LLG simulations to ensure a continuous energy spectrum of the whole system [40,56], can also be included in the SKFT-based derivation by using self-energy $\Sigma_k^{R/A}(\varepsilon)$ [52,72], which modifies the GFs of the central magnetic region in Fig. 1(b), $G_k^{R/A} = (\varepsilon - \varepsilon_k - \Sigma_k^{R/A})^{-1}$, where $\varepsilon_k = -2\gamma \cos k$.

The TDNEGF+LLG-computed trajectory $\mathbf{M}_1(t)$ of localized spin at site $n = 1$ is shown in Figs. 2(a) and 2(b) using two localized spins which are initially collinear and noncollinear, respectively. For the initially parallel [Fig. 2(a)] and antiparallel localized spins, we can extract Gilbert damping from such trajectories because $M_1^z(t) = \tanh\{\bar{\lambda}_{nn'}^{\text{1D}} B_{\text{ext}} t / [1 + (\bar{\lambda}_{nn'}^{\text{1D}})^2]\}$ [4,40], where the effective damping is given by $\bar{\lambda}_{nn'}^{\text{1D}} = \lambda_{00}^{\text{1D}} \pm \lambda_{nn'}^{\text{1D}}$ (+ for the parallel initial condition and – for the antiparallel initial condition). The nonlocality of this effective damping in Figs. 2(c) and 2(d) manifests as its oscillation with increasing separation of the two localized spins. The same result is predicted by the SKFT-derived formula [1D case in Eq. (10)], which remarkably closely traces

the numerically extracted $\bar{\lambda}_{nn'}^{\text{1D}}$ despite the approximations involved in the SKFT-based analytical derivation. Note also that the two localized spins remain collinear at all times t , but damping remains nonlocal. The feature missed by the SKFT-based formula is the decay of $\bar{\lambda}_{nn'}^{\text{1D}}$ with increasing $|\mathbf{r}_n - \mathbf{r}_{n'}|$, which is present in numerically extracted effective damping in Figs. 2(c) and 2(d). Note that effective damping is drastically reduced for antiparallel initial conditions due to the driving capabilities of the conduction electrons in addition to their dissipative nature. For noncollinear initial conditions, TDNEGF+LLG-computed trajectories become more complicated [Fig. 2(b)], so that we cannot extract effective damping $\lambda_{nn'}^{\text{1D}}$ akin to Figs. 2(c) and 2(d) for the collinear initial conditions.

D. Comparison of SKFT-derived formulas with the scattering theory [8] of uniform local Gilbert damping

The scattering theory of Gilbert damping α_G was formulated by studying a single-domain ferromagnet in contact with a thermal bath [8]. In such a setup, energy [8] and spin [61] pumped out of the system by time-dependent magnetization contain information about spin-relaxation-induced bulk [8,62] and interfacial [61] separable contributions to α_G , expressible in terms of the scattering matrix of a ferromagnetic layer attached to two semi-infinite NM leads. For collinear localized spins of the ferromagnet, precessing together as a macrospin, scattering-theory-derived α_G is a spatially uniform scalar which can be anisotropic [62]. Its expression is equivalent [62] to Kubo-type formulas [9,34–36] in the linear-response limit while offering an efficient algorithm for numerical first-principles calculations [24,25] that can include disorder and SOC on equal footing.

On the other hand, even if all localized spins are initially collinear, SKFT-derived extended LLG equation (9) predicts that due to nonlocal damping each localized spin will acquire a *distinct* $\mathbf{M}_n(t)$ trajectory, as demonstrated by solid red lines in Fig. 3(a). By feeding these trajectories, which are affected by nonlocal damping [1D case in Eq. (10)], into TDNEGF+LLG simulations, we can compute the spin current $I_R^S(t)$ pumped [56,57] into the right semi-infinite lead of the setup in Fig. 1(b) by the dynamics of $\mathbf{M}_n(t)$. A very similar result for pumped spin current is obtained [Fig. 3(b)] if we feed identical $\mathbf{M}_n(t)$ trajectories [black dashed line in Fig. 3(a)] from the conventional LLG equation with the Gilbert damping scalar parameter α_G , whose value is obtained by averaging the SKFT-derived nonlocal damping over the whole ferromagnet. This means that the scattering theory of Gilbert damping [8], which in this example is purely due to interfacial spin pumping [61] because of the lack of SOC and disorder (i.e., the absence of spin relaxation in the bulk), would predict a constant α_G that can be viewed only as the spatial average of SKFT-derived nonlocal and nonuniform $\lambda_{nn'}^{\text{1D}}$. In other words, Fig. 3 reveals that different types of microscopic magnetization dynamics $\mathbf{M}_n(t)$ can yield the same total spin angular momentum loss in the external circuit, which is therefore insufficient on its own to decipher the details (i.e., the proper form of the extended LLG equation) of the microscopic dynamics of local magnetization.

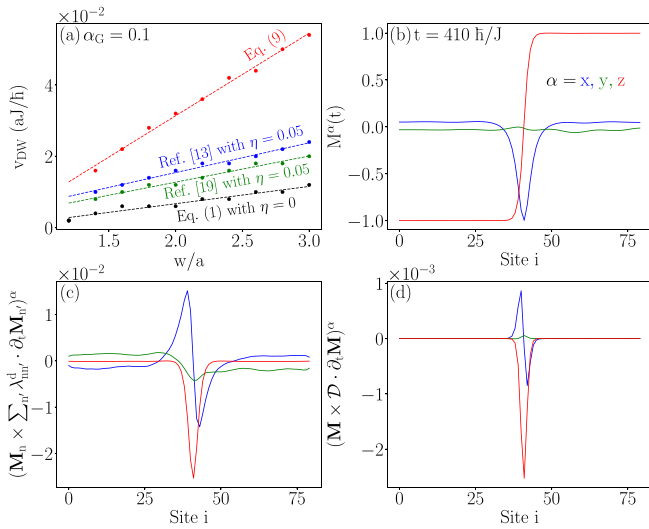


FIG. 4. (a) Comparison of magnetic DW velocity v_{DW} vs DW width w extracted from numerical simulations using the extended LLG equation (9) with SKFT-derived nonlocal damping [Eq. (10); red line], the extended LLG equation (1) with SMF-derived nonlocal damping from Ref. [13] [Eq. (2); blue line] or SMF-derived nonlocal damping from Ref. [19] [with an additional term compared to Ref. [13]; green line; see Eq. (14)], and the conventional LLG equation (1) with local Gilbert damping [i.e., $\eta = 0$ in Eq. (2); black line]. (b) Spatial profile of the DW within a quasi-1D ferromagnetic wire at time $t = 410 \hbar/J$, where J is the exchange coupling between \mathbf{M}_n at NN sites, as obtained from the SKFT-derived extended LLG equation (9) with nonlocal damping $\lambda_{nn'}^{2D}$ [Eq. (10)]. (c) and (d) The corresponding spatial profiles of nonlocal damping across the DW in (b) using the SKFT-derived expression [Eqs. (9) and (10)] and the SMF-derived [13] expression [second term on the right-hand side of Eq. (2)], respectively.

E. Comparison of SKFT-derived formulas with spin motive force theory [13] and [19] of nonlocal damping

The dynamics of noncollinear and noncoplanar magnetization textures, such as magnetic domain walls (DWs) and skyrmions, leads to pumping of charge and spin currents assumed to be captured by the SMF theory [16,73,74]. The excess angular momentum of dynamical localized spins carried away by the pumped spin current of electrons appears then as back-action torque [57] exerted by nonequilibrium electrons onto localized spins or, equivalently, nonlocal damping [13,17–19]. From this viewpoint, i.e., by using expressions for pumped spin current [13,17–19], a particular form for the nonlocal damping [second term on the RHS of Eq. (2)] was derived in Ref. [13] from the SMF theory and extended in Ref. [19] with an additional term while also invoking a number of intuitively justified but uncontrolled approximations.

In this section, we employ an example of a magnetic-field-driven DW [Fig. 4(b)] of width w within a quasi-1D ferromagnetic wire to compare its dynamics obtained by solving the extended LLG equation (1), which includes the nonlocal damping tensor [Eq. (2)] of Ref. [13], with the dynamics obtained by solving the SKFT-derived extended LLG equation (9) whose nonlocal damping is different from that in Ref. [13]. By neglecting nonlocal damping in Eq. (2), the

ferromagnetic DW velocity v_{DW} is found [75] to be directly proportional to Gilbert damping α_G , $v_{DW} \propto -B_{\text{ext}} w \alpha_G$, assuming a high external magnetic field B_{ext} and sufficiently small α_G . Thus, the value of α_G can be extracted by measuring the DW velocity. However, experiments found that α_G determined in this fashion can be up to three times larger than α_G extracted from the ferromagnetic resonance linewidth measurement scheme applied to the same material with uniform dynamical magnetization [10]. This is considered strong evidence of the importance of nonlocal damping in systems hosting noncollinear magnetization textures.

In order to properly compare the effect of two different expressions for the nonlocal damping, we use $\alpha_G = 0.1$ in Eq. (1), and we add the same standard local Gilbert damping term, $\alpha_G \mathbf{M}_n \times \partial_t \mathbf{M}_n$, to the SKFT-derived extended LLG equation (9). In addition, we set $\lambda_{00}^{2D} = \eta$ in Eq. (10), so that we can vary the same parameter η in all versions of the extended LLG [Eqs. (1), and (9)]. Note that we use $\lambda_{nn'}^{2D}$ in order to include realistic decay of nonlocal damping with increasing distance $|\mathbf{r}_n - \mathbf{r}_{n'}|$, thereby assuming a quasi-1D wire. By changing the width of the DW, the effective damping can be extracted from the DW velocity [Fig. 4(a)]. Figure 4(a) shows that $v_{DW} \propto w$ regardless of the specific version of nonlocal damping employed, and it increases in its presence—compare the red, blue, and green data points with the black ones obtained in the absence of nonlocal damping. Nevertheless, the clear distinction between the red data points and the blue and green data points indicates that our SKFT-derived nonlocal damping can be quite different from previously discussed SMF-derived nonlocal dampings [13,19], which are comparable regardless of the inclusion of the nonadiabatic terms. For example, the effective dampings extracted from the blue and green data points are $\mathcal{D} = 0.17$ and $\mathcal{D} = 0.15$, respectively, while $\lambda_{nn'}^{2D} = 0.48$. This distinction is further clarified by comparing spatial profiles of the SKFT-derived and SMF-derived nonlocal dampings in Figs. 4(c) and 4(d), respectively, at the instant of time used in Fig. 4(b). In particular, the profiles differ substantially in the out-of-DW-plane, or y , component, which is, together with the x component, an order of magnitude greater in the case of SKFT-derived nonlocal damping. In addition, the SKFT-derived nonlocal damping is *nonzero across the whole wire*, while the nonlocal damping in Eq. (2) is nonzero only within the DW width, where \mathbf{M}_n vectors are noncollinear [which is obvious from the presence of the spatial derivative in the second term on the RHS of Eq. (2)]. Thus, the spatial profile of SKFT-derived nonlocal damping in Fig. 4(c) illustrates how its nonzero value in the region outside the DW width does not require noncollinearity of \mathbf{M}_n vectors.

Since the SKFT-derived formulas are independently confirmed via numerically exact TDNEGF+LLG simulations in Figs. 2(c) and 2(d), we conclude that the previously derived [13] type of nonlocal damping [second term on the RHS of Eq. (2)] does not fully capture back-action of nonequilibrium conduction electrons on localized spins. This could be due to nonadiabatic corrections [16,19,74] to spin current pumped by dynamical noncollinear magnetization textures, which are present even in the absence of disorder and SOC [43]. One such correction was derived in Ref. [19] also using the spin current pumping approach, thereby adding a second nonlocal

damping term,

$$\eta \sum_{\beta'} [(\mathbf{M} \cdot \partial_{\beta'} \partial_t \mathbf{M}) \mathbf{M} \times \partial_{\beta'} \mathbf{M} - \mathbf{M} \times \partial_{\beta'}^2 \partial_t \mathbf{M}], \quad (14)$$

to the extended LLG equation (1). However, combined usage [green line in Fig. 4(a)] of both this term and the one in Eq. (2) as nonlocal damping still does not match the effect of SKFT-derived nonlocal damping [compare with the red line in Fig. 4(a)] on the magnetic DW. As demonstrated already in Fig. 3, the knowledge of total spin angular momentum loss carried away by pumped spin current [Fig. 3(b)], which is the key input in the derivations of Refs. [13,19], is, in general, *insufficient* to decipher the details of the microscopic dynamics and dissipation exhibited by localized spins [Fig. 3(a)] that pump such current.

F. Combining SKFT-derived nonlocal damping with first-principles calculations

Obtaining the closed-form expressions for the nonlocal damping tensor $\lambda_{nm'}$ in Secs. III A and III B was made possible by using simplistic model Hamiltonians and geometries. For realistic materials and more complicated geometries, in this section we provide general formulas which can be combined with DFT quantities and evaluated numerically.

Notably, the time-retarded dissipation kernel in Eq. (7), from which $\lambda_{nm'}$ is extracted, depends on the Keldysh GFs. The same GFs are also commonly used in first-principles calculations of the conventional Gilbert damping scalar parameter via Kubo-type formulas [29–33]. Specifically, the retarded and advanced GFs are obtained from first-principles Hamiltonians \hat{H}^{DFT} DFT as $\hat{G}^{R/A}(\epsilon) = [\epsilon - \hat{H}^{\text{DFT}} + \hat{\Sigma}^{R/A}(\epsilon)]^{-1}$. Here $\hat{\Sigma}^{R/A}(\epsilon)$ are the retarded and advanced self-energies [52,72] describing the escape rate of electrons into NM leads, allowing for open-system setups akin to the scattering-theory-derived formula for Gilbert damping [8,62] and its computational implementation with DFT Hamiltonians [24,25]. Since escape rates are encoded by the imaginary part of the self-energy, such calculations do not require the $i\eta$ imaginary parameter introduced by hand when using Kubo-type formulas [29–33] (where $\eta \rightarrow 0$ leads to unphysical divergent results [58–60]). Therefore, \hat{H}^{DFT} can be used as an input to compute the nonlocal damping tensor via the calculation of the GFs $\hat{G}^{R/A}(\epsilon)$ and the spectral function $\hat{A}(\epsilon) = i[\hat{G}^R(\epsilon) - \hat{G}^A(\epsilon)]$.

For these purposes, it is convenient to separate the nonlocal damping tensor into its symmetric and antisymmetric components, $\lambda_{nm'}^{\alpha\beta} = \lambda_{nm'}^{(\alpha\beta)} + \lambda_{nm'}^{[\alpha\beta]}$, where the parentheses (brackets) indicate that the encompassed indices have been (anti)symmetrized. They are given by

$$\lambda_{nm'}^{(\alpha\beta)} = -\frac{J_{sd}^2}{2\pi} \int d\epsilon \frac{\partial f}{\partial \epsilon} \text{Tr}_{\text{spin}} [\sigma^\alpha A_{nm'} \sigma^\beta A_{n'n}], \quad (15a)$$

$$\begin{aligned} \lambda_{nm'}^{[\alpha\beta]} = & -\frac{2J_{sd}^2}{\pi} \int d\epsilon \frac{\partial f}{\partial \epsilon} \text{Tr}_{\text{spin}} [\sigma^\alpha \text{Re} \hat{G}_{nm'}^R \sigma^\beta A_{n'n} - \sigma^\alpha A_{nm'} \sigma^\beta \text{Re} \hat{G}_{n'n}^R] \\ & + \frac{J_{sd}^2}{2\pi} \int d\epsilon (1 - 2f) \text{Tr}_{\text{spin}} \left[\sigma^\alpha \text{Re} \hat{G}_{nm'}^R \sigma^\beta \frac{\partial A_{n'n}}{\partial \epsilon} - \sigma^\alpha \frac{\partial A_{nm'}}{\partial \epsilon} \sigma^\beta \text{Re} \hat{G}_{n'n}^R \right], \end{aligned} \quad (15b)$$

where $f(\epsilon)$ is the Fermi function and the trace is taken in the spin space. The antisymmetric component either vanishes in the presence of inversion symmetry or is orders of magnitude smaller than the symmetric one. Therefore, it is absent in our results for simple models on hypercubic lattices. As such, the nonlocal damping tensors in Eqs. (10) and (13) are fully symmetric, and Eq. (15a) is a special case that occurs when we consider specific energy-momentum dispersions and assume zero temperature.

IV. CONCLUSIONS AND OUTLOOK

In conclusion, we derived a formula [Eqs. (15)] for magnetization damping of a metallic ferromagnet via a rigorous approach offered by the Schwinger-Keldysh nonequilibrium field theory [48] unexploited for this purpose. Our formulas could open a new route for calculations of the Gilbert damping of realistic materials by employing first-principles Hamiltonian \hat{H}^{DFT} from density functional theory as an input, as discussed in Sec. III F. Although a thorough numerical exploration of a small two-spin system based on SKFT was recently pursued in Ref. [54], our Eqs. (15) not only are

applicable for large systems of many localized spins but are also refined into readily computable expressions that depend on accessible quantities.

While traditional, Kubo linear response [9,30,34–36] or scattering theory [8] based derivations produce spatially uniform scalar α_G , SKFT-derived damping in Eqs. (15) is intrinsically nonlocal and nonuniform as it depends on the coordinates of local magnetization at two points in space, \mathbf{r}_n and $\mathbf{r}_{n'}$. In the cases of model Hamiltonians in one to three dimensions, we reduced Eqs. (15) to analytical expressions for magnetization damping [Eq. (10)], thereby making it possible to understand the consequences of such fundamental nonlocality and nonuniformity for local magnetization dynamics, such as the following: (i) Damping in Eq. (10) oscillates with the distance between \mathbf{r}_n and $\mathbf{r}_{n'}$, and the period of such oscillation is governed by the Fermi wave vector k_F [Figs. 1(c), 2(c), and 2(d)]. (ii) It always leads to nonuniform local magnetization dynamics [Fig. 3(a)], even though spin pumping from it can appear [Fig. 3(b)] as if it is driven by the usually analyzed [8,61] uniform local magnetization (or, equivalently, macrospin). (iii) When applied to noncollinear magnetic textures, such as DWs, it produces an order of magnitude larger

damping and therefore DW wall velocity than predicted by previously derived [13] nonlocal damping [second term on the RHS of Eq. (2)]. Remarkably, solutions of the SKFT-based extended LLG equation (9) are fully corroborated by numerically exact TDNEGF+LLG simulations [40,43,56,57] in one dimension, despite the fact that several approximations are employed in SKFT-based derivations. Finally, while conventional understanding of the origin of the Gilbert damping scalar parameter α_G requires SOC to be nonzero [22,23], our nonlocal damping is nonzero [Eq. (10)] even in the absence of SOC due to the inevitable delay [39,40] in electronic spin

responding to the motion of localized classical spins. For typical values of $J_{sd} \sim 0.1$ eV [76] and NN hopping parameter $\gamma \sim 1$ eV, the magnitude of the nonlocal damping is $\lambda_{nn'}^D \lesssim 0.01$, which is relevant even in metallic magnets with conventional local damping $\alpha_G \sim 0.01$ [10]. By switching SOC on, such nonlocal damping also becomes anisotropic [Eq. (13)].

ACKNOWLEDGMENT

This work was supported by the U.S. National Science Foundation (NSF), Grant No. ECCS 1922689.

- [1] L. D. Landau and E. M. Lifshitz, On the theory of the dispersion of magnetic permeability in ferromagnetic bodies, *Phys. Z. Sowjetunion* **8**, 153 (1935).
- [2] D. V. Berkov and J. Miltat, Spin-torque driven magnetization dynamics: Micromagnetic modeling, *J. Magn. Magn. Mater.* **320**, 1238 (2008).
- [3] S.-K. Kim, Micromagnetic computer simulations of spin waves in nanometre-scale patterned magnetic elements, *J. Phys. D* **43**, 264004 (2010).
- [4] R. Evans, W. Fan, P. Chureemart, T. Ostler, M. O. Ellis, and R. Chantrell, Atomistic spin model simulations of magnetic nanomaterials, *J. Phys.: Condens. Matter* **26**, 103202 (2014).
- [5] F. García-Gaítan and B. K. Nikolić, Fate of entanglement in magnetism under Lindbladian or non-Markovian dynamics and conditions for their transition to Landau-Lifshitz-Gilbert classical dynamics, [arXiv:2303.17596](https://arxiv.org/abs/2303.17596).
- [6] W. M. Saslow, Landau-Lifshitz or Gilbert damping? That is the question, *J. Appl. Phys.* **105**, 07D315 (2009).
- [7] T. Gilbert, A phenomenological theory of damping in ferromagnetic materials, *IEEE Trans. Magn.* **40**, 3443 (2004).
- [8] A. Brataas, Y. Tserkovnyak, and G. E. W. Bauer, Scattering theory of Gilbert damping, *Phys. Rev. Lett.* **101**, 037207 (2008).
- [9] D. Thonig and J. Henk, Gilbert damping tensor within the breathing Fermi surface model: Anisotropy and non-locality, *New J. Phys.* **16**, 013032 (2014).
- [10] T. Weindler, H. G. Bauer, R. Islinger, B. Boehm, J.-Y. Chauleau, and C. H. Back, Magnetic damping: Domain wall dynamics versus local ferromagnetic resonance, *Phys. Rev. Lett.* **113**, 237204 (2014).
- [11] L. Soumah, N. Beaulieu, L. Qassym, C. Carrétéro, E. Jacquet, R. Lebourgeois, J. B. Youssef, P. Bortolotti, V. Cros, and A. Anane, Ultra-low damping insulating magnetic thin films get perpendicular, *Nat. Commun.* **9**, 3355 (2018).
- [12] M. A. W. Schoen, D. Thonig, M. L. Schneider, T. J. Silva, H. T. Nembach, O. Eriksson, O. Karis, and J. M. Shaw, Ultra-low magnetic damping of a metallic ferromagnet, *Nat. Phys.* **12**, 839 (2016).
- [13] S. Zhang and S. S. L. Zhang, Generalization of the Landau-Lifshitz-Gilbert equation for conducting ferromagnets, *Phys. Rev. Lett.* **102**, 086601 (2009).
- [14] J. Foros, A. Brataas, Y. Tserkovnyak, and G. E. W. Bauer, Current-induced noise and damping in nonuniform ferromagnets, *Phys. Rev. B* **78**, 140402(R) (2008).
- [15] E. M. Hankiewicz, G. Vignale, and Y. Tserkovnyak, Inhomogeneous Gilbert damping from impurities and electron-electron interactions, *Phys. Rev. B* **78**, 020404(R) (2008).
- [16] Y. Tserkovnyak and M. Mecklenburg, Electron transport driven by nonequilibrium magnetic textures, *Phys. Rev. B* **77**, 134407 (2008).
- [17] Y. Tserkovnyak, E. M. Hankiewicz, and G. Vignale, Transverse spin diffusion in ferromagnets, *Phys. Rev. B* **79**, 094415 (2009).
- [18] K.-W. Kim, J.-H. Moon, K.-J. Lee, and H.-W. Lee, Prediction of giant spin motive force due to Rashba spin-orbit coupling, *Phys. Rev. Lett.* **108**, 217202 (2012).
- [19] H. Y. Yuan, Z. Yuan, K. Xia, and X. R. Wang, Influence of nonlocal damping on the field-driven domain wall motion, *Phys. Rev. B* **94**, 064415 (2016).
- [20] R. Verba, V. Tiberkevich, and A. Slavin, Damping of linear spin-wave modes in magnetic nanostructures: Local, nonlocal, and coordinate-dependent damping, *Phys. Rev. B* **98**, 104408 (2018).
- [21] S. Mankovsky, S. Wimmer, and H. Ebert, Gilbert damping in noncollinear magnetic systems, *Phys. Rev. B* **98**, 104406 (2018).
- [22] R. Mondal, M. Berritta, A. K. Nandy, and P. M. Oppeneer, Relativistic theory of magnetic inertia in ultrafast spin dynamics, *Phys. Rev. B* **96**, 024425 (2017).
- [23] M. C. Hickey and J. S. Moodera, Origin of intrinsic Gilbert damping, *Phys. Rev. Lett.* **102**, 137601 (2009).
- [24] A. A. Starikov, P. J. Kelly, A. Brataas, Y. Tserkovnyak, and G. E. W. Bauer, Unified first-principles study of Gilbert damping, spin-flip diffusion, and resistivity in transition metal alloys, *Phys. Rev. Lett.* **105**, 236601 (2010).
- [25] A. A. Starikov, Y. Liu, Z. Yuan, and P. J. Kelly, Calculating the transport properties of magnetic materials from first principles including thermal and alloy disorder, noncollinearity, and spin-orbit coupling, *Phys. Rev. B* **97**, 214415 (2018).
- [26] I. Garate and A. MacDonald, Gilbert damping in conducting ferromagnets. I. Kohn-Sham theory and atomic-scale inhomogeneity, *Phys. Rev. B* **79**, 064403 (2009).
- [27] I. Garate and A. MacDonald, Gilbert damping in conducting ferromagnets. II. Model tests of the torque-correlation formula, *Phys. Rev. B* **79**, 064404 (2009).
- [28] I. A. Ado, P. M. Ostrovsky, and M. Titov, Anisotropy of spin-transfer torques and Gilbert damping induced by Rashba coupling, *Phys. Rev. B* **101**, 085405 (2020).
- [29] K. Gilmore, Y. U. Idzerda, and M. D. Stiles, Identification of the dominant precession-damping mechanism in Fe, Co, and Ni by first-principles calculations, *Phys. Rev. Lett.* **99**, 027204 (2007).
- [30] H. Ebert, S. Mankovsky, D. Ködderitzsch, and P. J. Kelly, *Ab initio* calculation of the Gilbert damping parameter via

- the linear response formalism, *Phys. Rev. Lett.* **107**, 066603 (2011).
- [31] S. Mankovsky, D. Ködderitzsch, G. Woltersdorf, and H. Ebert, First-principles calculation of the Gilbert damping parameter via the linear response formalism with application to magnetic transition metals and alloys, *Phys. Rev. B* **87**, 014430 (2013).
- [32] Y. S. Hou and R. Q. Wu, Strongly enhanced Gilbert damping in 3d transition-metal ferromagnet monolayers in contact with the topological insulator Bi₂Se₃, *Phys. Rev. Appl.* **11**, 054032 (2019).
- [33] F. S. M. Guimarães, J. R. Suckert, J. Chico, J. Bouaziz, M. dos Santos Dias, and S. Lounis, Comparative study of methodologies to compute the intrinsic Gilbert damping: Interrelations, validity and physical consequences, *J. Phys.: Condens. Matter* **31**, 255802 (2019).
- [34] V. Kamberský, On ferromagnetic resonance damping in metals, *Czech. J. Phys.* **26**, 1366 (1976).
- [35] V. Kamberský, FMR linewidth and disorder in metals, *Czech. J. Phys.* **34**, 1111 (1984).
- [36] V. Kamberský, Spin-orbital Gilbert damping in common magnetic metals, *Phys. Rev. B* **76**, 134416 (2007).
- [37] V. G. Bar'yakhtar, Phenomenological description of relaxation processes in magnetic materials, *Sov. Phys. JETP* **60**, 863 (1984).
- [38] Y. Li and W. E. Bailey, Wave-number-dependent Gilbert damping in metallic ferromagnets, *Phys. Rev. Lett.* **116**, 117602 (2016).
- [39] M. Sayad and M. Potthoff, Spin dynamics and relaxation in the classical-spin Kondo-impurity model beyond the Landau-Lifshitz-Gilbert equation, *New J. Phys.* **17**, 113058 (2015).
- [40] U. Bajpai and B. K. Nikolić, Time-retarded damping and magnetic inertia in the Landau-Lifshitz-Gilbert equation self-consistently coupled to electronic time-dependent nonequilibrium Green functions, *Phys. Rev. B* **99**, 134409 (2019).
- [41] D. Thonig, J. Henk, and O. Eriksson, Gilbert-like damping caused by time retardation in atomistic magnetization dynamics, *Phys. Rev. B* **92**, 104403 (2015).
- [42] D. Ralph and M. Stiles, Spin transfer torques, *J. Magn. Magn. Mater.* **320**, 1190 (2008).
- [43] A. Suresh, U. Bajpai, and B. K. Nikolić, Magnon-driven chiral charge and spin pumping and electron-magnon scattering from time-dependent quantum transport combined with classical atomistic spin dynamics, *Phys. Rev. B* **101**, 214412 (2020).
- [44] M. V. Berry and J. M. Robbins, Chaotic classical and half-classical adiabatic reactions: Geometric magnetism and deterministic friction, *Proc. R. Soc. London, Ser. A* **442**, 659 (1993).
- [45] M. Campisi, S. Denisov, and P. Hänggi, Geometric magnetism in open quantum systems, *Phys. Rev. A* **86**, 032114 (2012).
- [46] M. Thomas, T. Karzig, S. V. Kusminskiy, G. Zaránd, and F. von Oppen, Scattering theory of adiabatic reaction forces due to out-of-equilibrium quantum environments, *Phys. Rev. B* **86**, 195419 (2012).
- [47] U. Bajpai and B. K. Nikolić, Spintronics meets nonadiabatic molecular dynamics: Geometric spin torque and damping on dynamical classical magnetic texture due to an electronic open quantum system, *Phys. Rev. Lett.* **125**, 187202 (2020).
- [48] A. Kamenev, *Field Theory of Non-equilibrium Systems* (Cambridge University Press, Cambridge, 2023).
- [49] M. Onoda and N. Nagaosa, Dynamics of localized spins coupled to the conduction electrons with charge and spin currents, *Phys. Rev. Lett.* **96**, 066603 (2006).
- [50] Y. Rikitake and H. Imamura, Decoherence of localized spins interacting via RKKY interaction, *Phys. Rev. B* **72**, 033308 (2005).
- [51] J. Fransson, Dynamical exchange interaction between localized spins out of equilibrium, *Phys. Rev. B* **82**, 180411(R) (2010).
- [52] A. S. Núñez and R. A. Duine, Effective temperature and Gilbert damping of a current-driven localized spin, *Phys. Rev. B* **77**, 054401 (2008).
- [53] S. Díaz and Á. S. Núñez, Current-induced exchange interactions and effective temperature in localized moment systems, *J. Phys.: Condens. Matter* **24**, 116001 (2012).
- [54] S. Leiva M., S. A. Díaz, and A. S. Nunez, Origin of the magnetoelectric couplings in the spin dynamics of molecular magnets, *Phys. Rev. B* **107**, 094401 (2023).
- [55] A. Rebei, W. N. G. Hitchon, and G. J. Parker, *s-d*-type exchange interactions in inhomogeneous ferromagnets, *Phys. Rev. B* **72**, 064408 (2005).
- [56] M. D. Petrović, B. S. Popescu, P. Plecháč, and B. K. Nikolić, Spin and charge pumping by current-driven magnetic domain wall motion: A self-consistent multiscale time-dependent-quantum/time-dependent-classical approach, *Phys. Rev. Appl.* **10**, 054038 (2018).
- [57] M. D. Petrović, U. Bajpai, P. Plecháč, and B. K. Nikolić, Annihilation of topological solitons in magnetism with spin-wave burst finale: Role of nonequilibrium electrons causing nonlocal damping and spin pumping over ultrabroadband frequency range, *Phys. Rev. B* **104**, L020407 (2021).
- [58] A. T. Costa and R. B. Muniz, Breakdown of the adiabatic approach for magnetization damping in metallic ferromagnets, *Phys. Rev. B* **92**, 014419 (2015).
- [59] D. M. Edwards, The absence of intraband scattering in a consistent theory of Gilbert damping in pure metallic ferromagnets, *J. Phys.: Condens. Matter* **28**, 086004 (2016).
- [60] F. Mahfouzi, J. Kim, and N. Kioussis, Intrinsic damping phenomena from quantum to classical magnets: An *ab initio* study of Gilbert damping in a Pt/Co bilayer, *Phys. Rev. B* **96**, 214421 (2017).
- [61] Y. Tserkovnyak, A. Brataas, G. E. W. Bauer, and B. I. Halperin, Nonlocal magnetization dynamics in ferromagnetic heterostructures, *Rev. Mod. Phys.* **77**, 1375 (2005).
- [62] A. Brataas, Y. Tserkovnyak, and G. E. W. Bauer, Magnetization dissipation in ferromagnets from scattering theory, *Phys. Rev. B* **84**, 054416 (2011).
- [63] N. Nagaosa, J. Sinova, S. Onoda, A. H. MacDonald, and N. P. Ong, Anomalous Hall effect, *Rev. Mod. Phys.* **82**, 1539 (2010).
- [64] A. Altland and B. Simons, *Condensed Matter Field Theory* (Cambridge University Press, Cambridge, 2023).
- [65] A. Shnirman, Y. Gefen, A. Saha, I. S. Burmistrov, M. N. Kiselev, and A. Altland, Geometric quantum noise of spin, *Phys. Rev. Lett.* **114**, 176806 (2015).
- [66] R. C. Verstraten, T. Ludwig, R. A. Duine, and C. Morais Smith, Fractional Landau-Lifshitz-Gilbert equation, *Phys. Rev. Res.* **5**, 033128 (2023).
- [67] H. M. Hurst, V. Galitski, and T. T. Heikkilä, Electron-induced massive dynamics of magnetic domain walls, *Phys. Rev. B* **101**, 054407 (2020).

- [68] A. Manchon, H. C. Koo, J. Nitta, S. M. Frolov, and R. A. Duine, New perspectives for Rashba spin–orbit coupling, *Nat. Mater.* **14**, 871 (2015).
- [69] A. A. Baker, A. I. Figueroa, C. J. Love, S. A. Cavill, T. Hesjedal, and G. van der Laan, Anisotropic absorption of pure spin currents, *Phys. Rev. Lett.* **116**, 047201 (2016).
- [70] M. Fähnle, D. Steiauf, and J. Seib, The Gilbert equation revisited: Anisotropic and nonlocal damping of magnetization dynamics, *J. Phys. D* **41**, 164014 (2008).
- [71] E. Montoya, B. Heinrich, and E. Girt, Quantum well state induced oscillation of pure spin currents in Fe/Au/Pd(001) systems, *Phys. Rev. Lett.* **113**, 136601 (2014).
- [72] D. Ryndyk, *Theory of Quantum Transport at Nanoscale* (Springer, Cham, 2016).
- [73] S. E. Barnes and S. Maekawa, Generalization of Faraday’s law to include nonconservative spin forces, *Phys. Rev. Lett.* **98**, 246601 (2007).
- [74] R. A. Duine, Effects of nonadiabaticity on the voltage generated by a moving domain wall, *Phys. Rev. B* **79**, 014407 (2009).
- [75] G. Tatara, Effective gauge field theory of spintronics, *Phys. E (Amsterdam, Neth.)* **106**, 208 (2019).
- [76] R. L. Cooper and E. A. Uehling, Ferromagnetic resonance and spin diffusion in supermalloy, *Phys. Rev.* **164**, 662 (1967).